Int. J. Multiphase Flow, Vol. 4, pp. 487–496. Pergamon/Elsevier, 1978. Printed in Great Britain

THREE-DIMENSIONAL SURFACE CHARACTERISTICS OF A FALLING LIQUID FILM

RONALD P. SALAZAR and EKKEHARD MARSCHALL

Mechanical and Environmental Engineering Department, University of California, Santa Barbara, CA 93106, U.S.A.

(*Received* 2 *December* 1976)

Abstract—Optical methods are described for examining the three-dimensional character of waves on a falling liquid film. This involved monitoring the motion of the local film surface normal through the use of laser beam refraction. The wavy motion was found to be primarily of a two-dimensional nature only for *Re* (equal to $4Q/\nu$) less than 1500.

Surface characteristics were examined for Reynolds numbers from 217 to 4030 and for different distances along the direction of flow.

INTRODUCTION

The wave characteristics of falling liquid film flow have been the subject of theoretical and experimental studies for many years. Fulford (1964) lists papers on film flow beginning with that of Hopf (1910), who made observations of film thickness, surface velocity and wave formation in gravity induced film flow.†

Throughout nearly all these studies we find the assumption, either expressed or implied, that the motion of falling film waves is strictly two-dimensional. However for any given Reynolds number this assumption may not be accurate. Indeed if we observe the surface of a typical wavy falling film we are struck immediately by the irregularity and three-dimensionality of the surface waves.

The objective of this study has been to examine this three-dimensionality through the use of new optical methods for monitoring the motion of the local film surface normal **n**. This should help to determine the circumstances under which falling liquid film flow can be considered a two-dimensional process.

An additional goal was to examine the dependence of surface characteristics not only on Reynolds number but also on distance in the direction of the flow. To date only Portalski & Clegg (1972) and very few others have used a similar approach.

METHODS

The liquid used in these experiments was distilled water at 24°C. It was distributed evenly across a small reservoir from which it flowed over the machined knife-edge and down a vertical Plexiglas plate, 35.67 cm wide and 155 cm in length. The sides of the plate were bordered by very smooth 1.27 cm thick Plexiglas sledges. The flow rate could be adjusted to provide Reynolds numbers ($4Q/\nu$ where Q is the volumetric flowrate per unit length across the flow and ν is kinematic viscosity) anywhere between 217 and 4030.

The basic idea of this optical method is to examine the refraction of a laser beam as it passes through a wavy film on a vertical Plexiglas plate and relate this motion to that of the surface normal. As shown in figure 1 the laser beam‡ passes through the Plexiglas plate through the water film, and is refracted at the water–air interface. Waves on the film surface pass through the beam which traces out a pattern on whatever surface it strikes. Each point along this line corresponds uniquely to a particular direction of **n**, hence a particular surface inclination angle. If the passing waves are two-dimensional, the trace will be a single straight line, while three-dimensional waves will result in more complicated patterns. When the surface is flat we observe only a single spot.

†More recently theoretical approaches were reviewed by Dukler (1972) and experimental methods by Hewitt (1972).
‡This is produced by an Optics Technology Model 195 He–Ne laser with a beam diameter in water of about 2 mm.

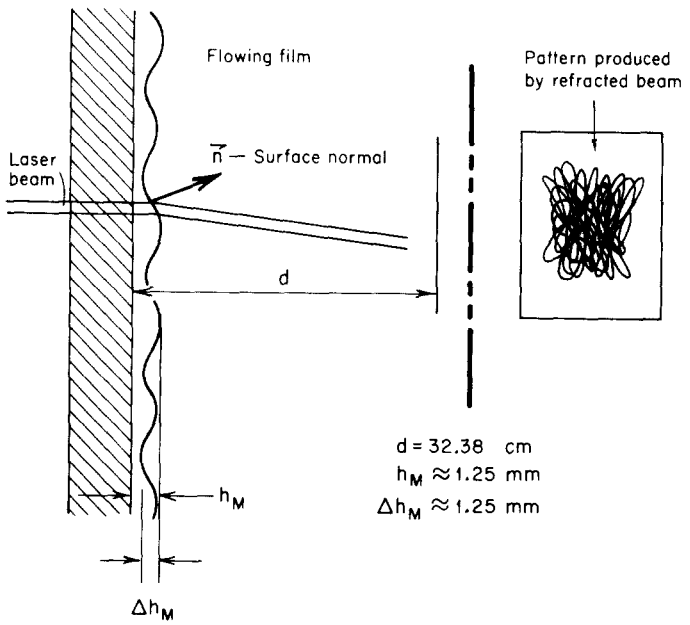

Figure 1. Refraction of laser beam due to waves.

Two methods were used to study the refracted beam patterns. The first involves placing a screen of thin white paper in front of the beam taking time exposure photographs of the pattern produced on it from the side opposite the laser beam. One of these might appear as in figure 1. The second method employs a 100-element array of light sensitive diodes† to estimate the relative probabilities (or frequency of occurrence) of different angles of surface inclination. This is done by comparing the amounts of optical power delivered to individual photodiodes. For example, a photodiode placed near the center of the refracted beam pattern in figure 1 would certainly be struck by the laser beam more often than one near the edge. Since the laser is the only source of illumination for the photodiodes, their average outputs tell us how much time the laser beam spends on one photodiode face relative to the other. This in turn supplies us with information on the likelihood of one direction of surface normal **n** relative to another.

If we were to make a three-dimensional figure plotting time-averaged light intensity as a function of position on the screen where the refracted patterns are made, it would appear similar to those in figure 2. The first of these (2-a) is the average intensity pattern produced by purely two-dimensional waves while the second (2-b) is produced by a very rough liquid surface. The laser spot seen on the screen moves back and forth in only one dimension in the former and randomly in two dimensions in the latter, producing a three-dimensional average intensity contour. For the purposes of this illustration we assumed that the beam will strike the center of the screen very often and the area near the edge very seldom. The result is a high average intensity near the center and lower average intensity as we moved outward.

By comparing average intensity at any two points in the x–y plane, where the x axis is parallel to the flow direction, we have an estimate of the relative probabilities of the surface angles which would cause the laser beam to strike these particular points.

The first method mentioned above amounts to looking at figure 2 in the z-direction. What we see on the photographs is constant intensity line 4 near the base of the surface. The height of this line $\bar{I}_0$, is determined by the sensitivity of the photographic system.

The array of light sensitive diodes employed in the second method is mounted on a stage that can be rotated through 360° about one end of the array. For this experiment it was set at three positions (shown in figure 3) and the output signals of selected diodes were averaged over

†These devices produce a certain amount of current per watt of optical power striking their active area. Each diode has active areas of 0.254 mm × 0.493 mm. The spacing between the active area is 0.101 mm.

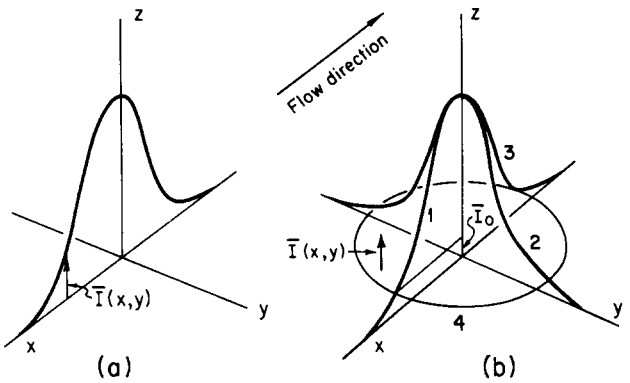

Intensity contours produced by
(a) Two dimensional wave motion
(b) Three dimensional wave motion

Figure 2. Refracted intensity distributions due to waves.

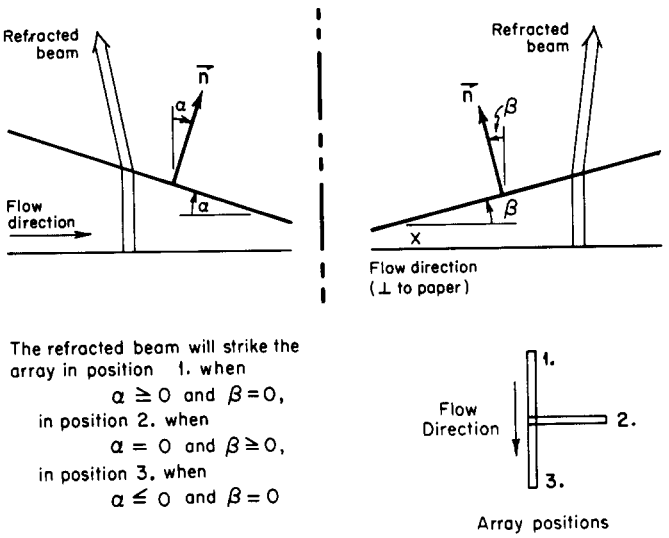

The refracted beam will strike the array in position 1. when
$\alpha \geq 0$ and $\beta = 0$,
in position 2. when
$\alpha = 0$ and $\beta \geq 0$,
in position 3. when
$\alpha \leq 0$ and $\beta = 0$

Figure 3. Laser beam refraction due to slanted film surface.

a specified time. In figure 3 are shown the surface angles which must occur for the beam to strike the array in any one of these three positions.

Referring again to figure 2, we see that the second method amounts to viewing the $\bar{I}(x,y)$ surface contour in the x-direction and in the y-direction. That is, we find the shapes of curves 1, 2 and 3 in figure 2 when the array is set in positions 1, 2 and 3 respectively. The final result is a three-dimensional view of the surface.

There are two small sources of ambiguity in this measurement. One is the finite size of the diode faces, and the other is the changing film thickness (figure 1). These will clearly be insignificant since d, the distance from the Plexiglas plate to the photodiode array (≈ 32 cm), is much greater than h_M, the maximum film thickness (~ 1 mm), Δh_M, the maximum variation in film thickness (~ 1 mm), and the diode active area dimensions.

Readings were taken at the diodes shown in figure 4. The curve for this figure is produced when the surface is flat and the beam is centered on photodiode number 1. The succeeding diodes follow in order up to number 97 which is a distance of 34.1 mm away from number 1. Each photodiode output went through a preamplifier (United Detector Tech. 101A) to insure maximum linearity and was averaged over 100 s by a Hewlett-Packard 2410 integrating digital voltmeter.

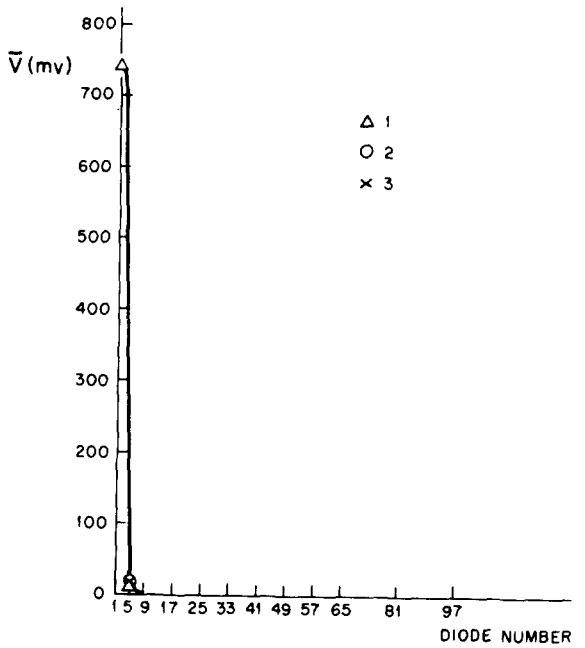

Figure 4. Refracted intensity distribution for a flat film.

The diode responsivities are all within 8% of No. 1. It was decided to use the outputs as is and make no corrections for different responsivities due to the generally large differences between average diode outputs.†

To keep the diodes within their linear range (output current vs input power), a neutron density filter which transmits 6.4% of the incident power was used to attenuate the 2 mW laser beam.

RESULTS

Measurements were taken at four locations in the flow direction and at six Reynolds numbers. Only those in a region of wavy flow are meaningful, so the result was 16 different measurements as follows:

	Measurement location (distance from leading edge)	Reynolds Nos.
Station 1	8.4 cm	217
Station 2	27 cm	217, 600, 1000
Station 3	64.1 cm	217, 600, 1000, 1955, 3050, 4030
Station 4	133.7 cm	217, 600, 1000, 1955, 3050, 4030

Typical results of these measurements are shown in figures 5–7 with the same scales as in figure 4. Curves 1, 2, and 3 are those shown in figure 2; the photographs contain curve 4. The surface angles corresponding to each photodiode are given in table 1. All readings are in millivolts and have been normalized for differences in laser power from one measurement to the next. Only those readings for which the intensity was greater than 1% of that at diode No. 1 are shown here.

†A similar problem arises due to changes in transmitted laser intensity with changing surface angle. That is, the intensity of the refracted laser beam will be a function of the film surface inclination. However, this effect is also small. The surface angle corresponding to diode number 97 is about 17.6° and for this angle the transmitted intensity will have arisen only a few per cent. Another small effect is decreasing diode responsivity with increasing incidence angle of the beam on the diode face. But this effect is only about 2% for an incidence angle of 6° on number 97.

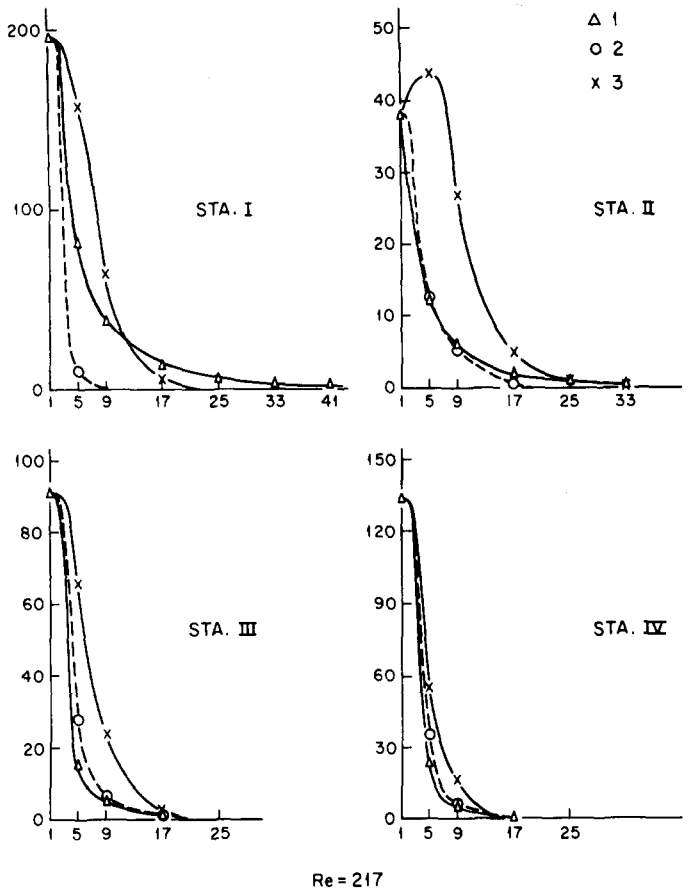

Figure 5a. Time-average refracted intensity distribution for $Re = 217$. (Scales as in figure 4.)

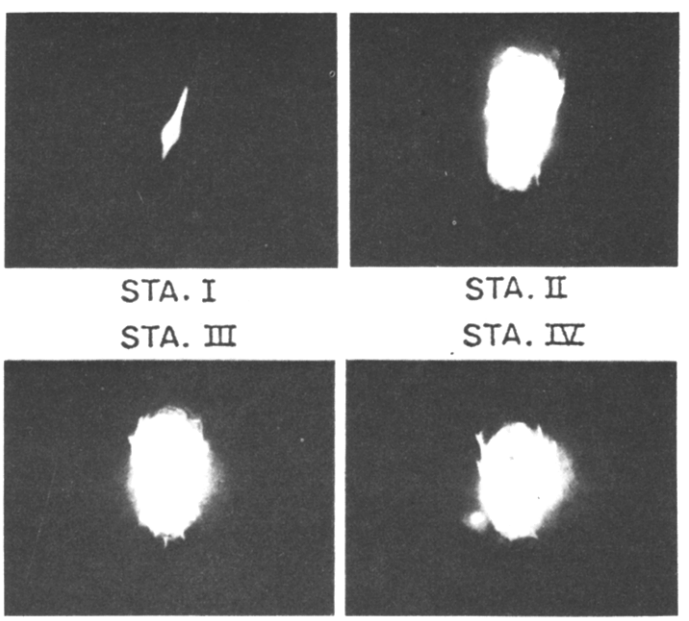

Figure 5b. Shape of constant intensity line 4 for $Re = 217$.

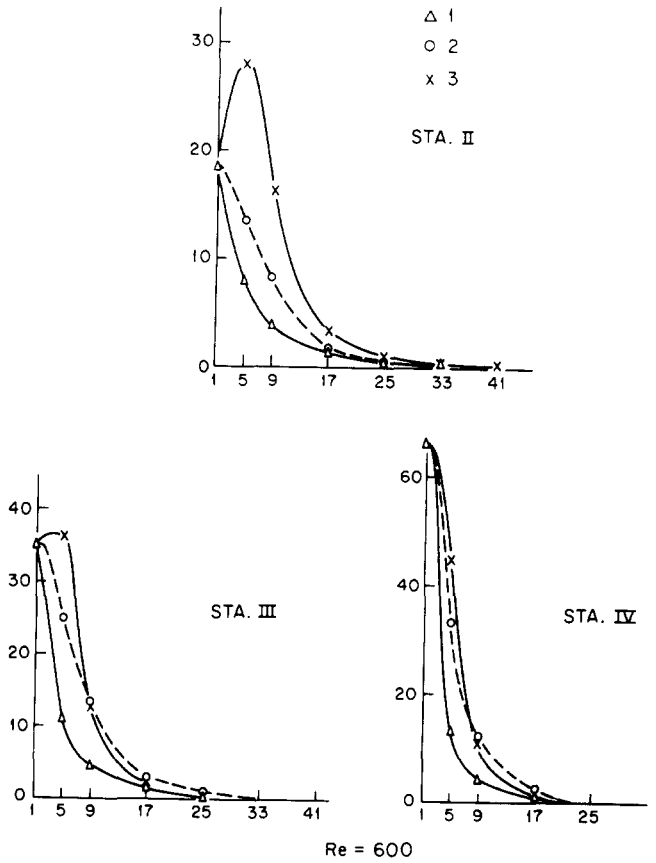

Figure 6a. Time-average refracted intensity distribution for $Re = 600$. (Scales as in figure 4.)

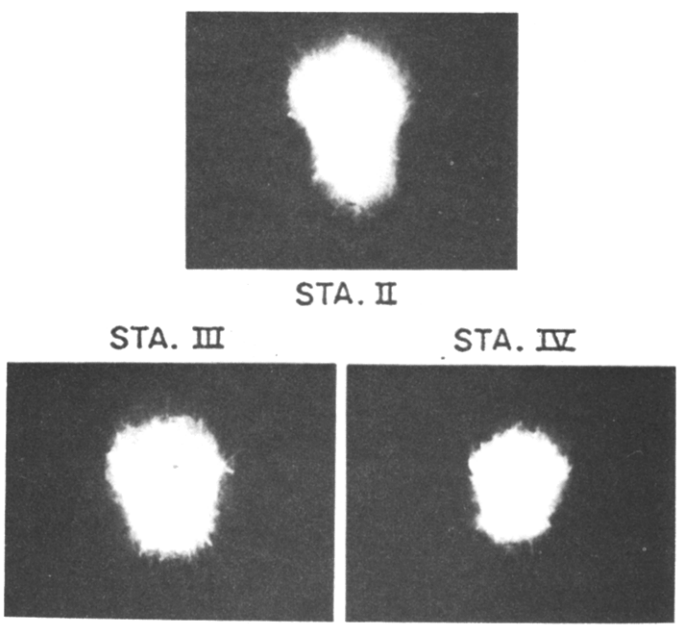

Figure 6b. Shape of constant intensity line 4 for $Re = 600$.

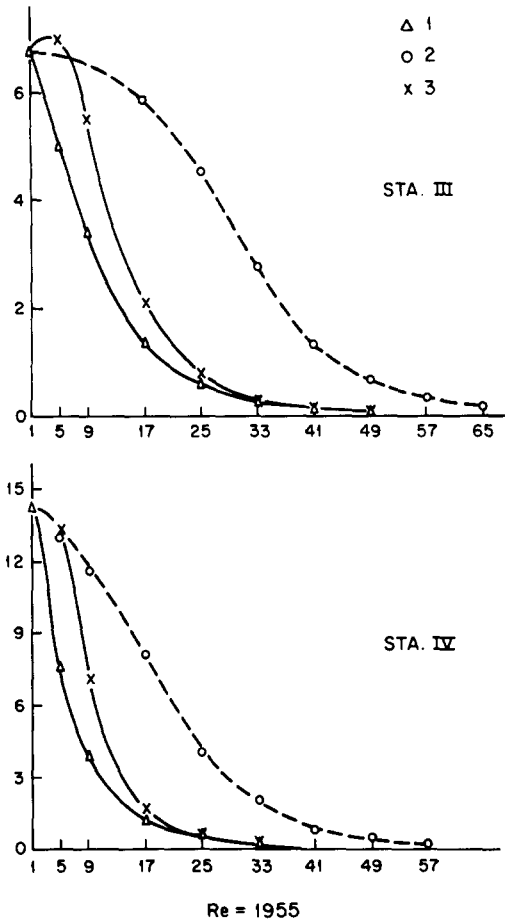

(a)

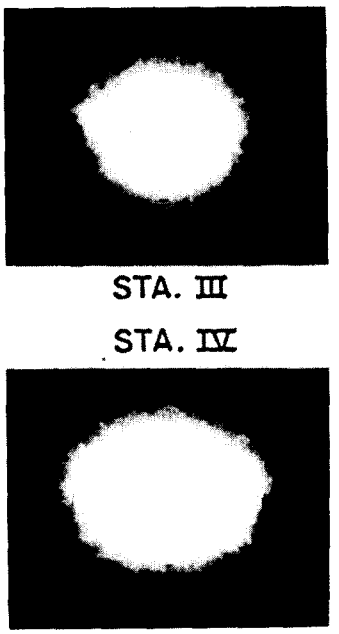

(b)

Figure 7a. Time-average refracted intensity distribution for $Re = 1955$. (Scales as in figure 4).

Figure 7b. Shape of constant intensity line 4 for $Re = 1955$.

Table 1.

Diode	Surface angle† (α or β)
1	0°
5	0.758°
9	1.515°
17	3.058°
25	4.566°
33	6.067°
41	7.559°
49	9.071°
57	10.539°
65	11.994°
81	14.851°
97	17.631°

†The relation between diode position and surface angle is given by

$$\alpha \text{ or } \beta = \tan^{-1}\left(\frac{\sin\theta_{di}}{(n_1/n_2)-\cos\theta_{di}}\right),$$

where α or β = surface inclination angle, θ_{di} = deflection angle of laser beam as it exits the water, n_1 = index of refraction of water, n_2 = index of refraction of air.

In table 2 are listed the maximum values of the surface angles α and β shown in figure 3. These were obtained by visual observation of the maximum deflection of the refracted laser beam on a sheet of white paper using the relation between beam deflection angle θ_d and surface angle.

It should be noted that these are approximate outside limits on the surface angles α and β. The actual maximum at any Reynolds number could easily be slightly less (say 2° and 4°) but should rarely, if ever, be greater.

Table 2. Maximum values of surface angles α and β

	Re	α_{M+}	β_M	α_{M-}
Station 2	217	24.371°	13.330°	19.497°
	600	38.534°	24.371°	32.713°
	1000	38.534°	24.371°	34.060°
Section 3	217	24.371°	13.330°	19.497°
	600	38.534°	24.371°	32.713°
	1000	42.457°	32.713°	35.901°
	1955	42.457°	32.713°	35.901°
	3050	42.457°	35.901°	38.534°
	4030	45.968°	35.901°	40.695°
Station 4	217	24.371°	13.330°	32.713°
	600	38.534°	24.371°	32.713°
	1000	42.457°	32.715°	38.534°
	1955	43.887°	35.901°	38.534°
	3050	43.887°	35.901°	38.534°
	4030	45.968°	35.901°	40.695°

α_{M+} = maximum positive value of α, β_M = maximum value of β, α_{M-} = maximum negative value of α.

The numbers of table 2 indicate that the waves do not change very much in shape as they travel down the plate. Of course few of these measurements are in the regions of very regular wave motion where the waves are just being formed. It would not be surprising if the wave shapes in this region were somewhat different from those that occur later. However, it appears that after a certain time the waves achieve a stable shape which doesn't change much thereafter. An example of this behavior can be seen at $Re = 1000$. The first measurements at station 2 are near the area where waves first appear at this Reynolds number. We see that the maximum surface angles increase between stations 2 and 3 and then change only slightly between 3 and 4.

A quick glance through the figures 5–7 gives some idea of the inadequacy of a two-dimensional model for falling film wave motion. Only at the lowest Reynolds number (217) does the wave motion appear to be very strongly two-dimensional. All higher Reynolds numbers are characterized by large values of the surface angle α. At the highest Reynolds numbers the photographs suggest almost totally random variations in surface angle.

There appears to be a qualitative change taking place between the Reynolds numbers below about 1500 and those above.† Below this number the photographs indicate that the refracted beam generally moves in an up and down motion, though increased spreading occurs for greater distances along the plate and higher flow rates. Above 1500 no such pattern is apparent, indicative of a highly irregular surface. This indicates that below 1500 an assumption of mostly two-dimensional wave motion might still be reasonable.

The reason for the spreading of the patterns in the y-direction can be seen upon careful observation of the wave motion. What apparently occurs is this: the flat region of no waves is

†The critical Reynolds number marking the transition to turbulent flow is generally regarded to be around 1500. Values have been reported over a wide range but most are in the area from 1000 to 1600. No doubt the transition occurs gradually throughout and even beyond this range.

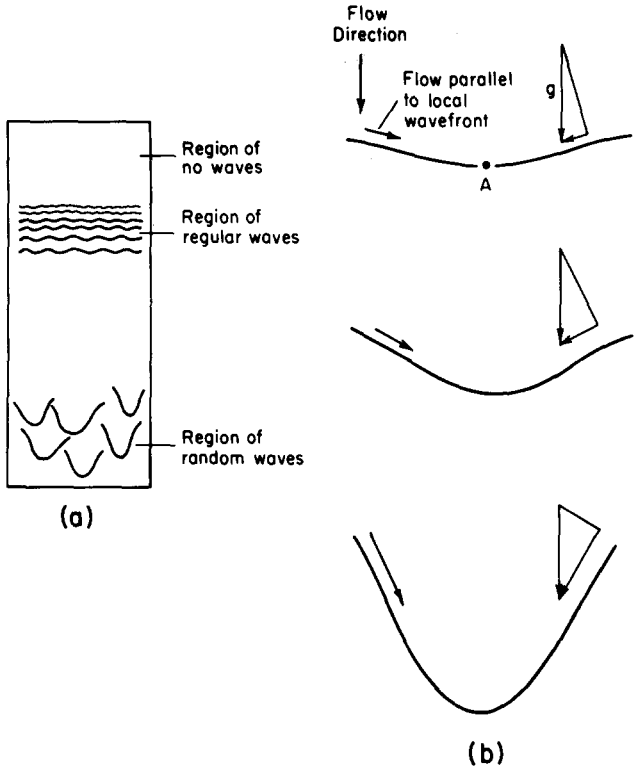

Figure 8. Deformation of wavefronts in the flow direction.

followed by an area of very regular short wavelength motion as shown in figure 8a. Due to slight variations in flow rate in the y-direction, the wave fronts are not exactly straight but are slightly rippled. Now looking closely at one of these wavefronts, we find the situation in figure 8b. The local wavefront is not exactly horizontal but slightly tilted. Therefore gravity, acting vertically, has a small component parallel to the wavefront. This induces a flow in this direction, causing water to build up behind the point A and causing increasing distortion of the wavefronts along the x-direction. The regular waves thus evolve into a group of independent masses of liquid in which is contained a large part of the total flow. This effect is more pronounced the higher the Reynolds number leading to the extremely irregular surface shapes suggested by the refracted beam patterns mentioned previously.

This evolution is apparent in figure 5a for $Re = 217$. Here we see the points in curve 2 representing angle β growing larger between stations 1 and 2 and then staying about the same thereafter. The change that we note between stations 2, 3, and 4 is a steady increase in the average voltage at diode 1, corresponding to a surface slope of zero. What this seems to indicate is that the waves are accelerating as they travel down the plate. Thus, the flat areas between waves are growing larger and the waves are becoming farther and farther apart.

CONCLUSIONS

To sum up, we can make the following statements about the wave motion as shown by the refraction patterns:

(1) The average intensity reading at diode 1 ($\alpha = \beta = 0°$) increases steadily after the wave motion is fully developed for all Reynolds numbers (from stations 2 to 4 for 217 and 600; from stations 3 to 4 for 1000 to 4030) indicating that the waves are becoming farther apart as they travel down the plate.

(2) Higher values for curve 3, which represents the back parts of waves at diodes 5–17 ($\alpha = -1°$ to $-4°$) indicate asymmetry of the waves, that is, long gently sloping tails and shorter,

steeper fronts. This is also indicated by the maximum angle measurements in that the maximum positive values of α are always of greater magnitude than the maximum negative values.

In the photographs wave asymmetry is shown by the fact that all of the patterns have a top part somewhat larger, that is, more spread out than the bottom part. The refracted beam struck the upper part of these patterns when surface angle α (figure 3) was positive, that is, on the front part of the waves, indicating short, steep fronts and longer, less steep tails.

(3) Wave motion appears primarily although not exclusively two-dimensional for all Reynolds numbers below the turbulent region (~ 1500). Above this, curve 2 spreads out and the pattern shown in the photographs becomes wider than it is long, indicating a very irregular surface. A large part of this irregularity may not be exactly like the waves of the laminar region but rather random surface fluctuations due to turbulent fluctuations within the flow.

(4) The surface is still flat in the area near the entrance even when the flow is in the turbulent region of Reynolds numbers.

Acknowledgement—This work was supported by National Science Foundation Grant GK-35797.

REFERENCES

DUKLER, A. E. 1972 Characterization, effects, and modeling of the wavy gas-liquid interface. *Progress in Heat and Mass Transfer*, Vol. 6, pp. 207–234. Pergamon Press, New York.

FULFORD, G. D. 1964 The flow of liquids in thin films. *Advances in Chemical Engineering*, Vol. 5, pp. 151–236. Academic Press, New York.

HEWITT, G. F. 1972 The role of experiments in two-phase systems with particular reference to measurement techniques. *Progress in Heat and Mass Transfer*, Vol. 6, pp. 295–343. Pergamon Press, New York.

HOPF, L. 1910 Turbulenz bei einem Flusse. *Am. Physik* **32**, 777–784.

PORTALSKI, S. & CLEGG A. J. 1972 An experimental study of wave inception on falling liquid films. *Chem. Engr. Sci.* **27**, 1257–1265.